Paper:

Damage Assessment of Road Bridges Subjected to the 2011 Tohoku Pacific Earthquake Tsunami

Gaku Shoji*,† **and Tomoharu Nakamura****

*Division of Engineering Mechanics and Energy, Faculty of Engineering, Information and Systems, University of Tsukuba
1-1-1 Tennodai, Tsukuba, Ibaraki 305-8573, Japan
†Corresponding author, E-mail: gshoji@kz.tuskuba.ac.jp
**Former Graduate Student, Graduate School of Systems and Information Engineering, University of Tsukuba, Ibaraki, Japan
[Received August 11, 2016; accepted December 8, 2016]

The authors assessed the tsunami damage to a girder-type road bridge, focusing on a washed-away deck that failed during the 2011 Tohoku Pacific earthquake tsunami. The inundation depth, ratio of inundation depth to girder elevation, and flow velocity were used as the three indices of the tsunami wave load acting on a road bridge deck. A gently shaped tsunami waveform was selected at a wave-front with a water surface level increase rate of less than 2.0 m/min. The damage ratio was computed for the above three indices, as defined by the number of washed-away bridges divided by the total number of bridges exposed to the tsunami. Based on statistical analysis for the damage ratio data, damage functions using the three indices were proposed. In addition, the spatial distribution of physical wash-away damage to road bridges by the anticipated Nankai Trough earthquake tsunami was shown by applying the derived damage functions.

Keywords: the 2011 Tohoku Pacific Earthquake Tsunami, road bridge, inundation depth, damage function, the Nankai Trough earthquake tsunami

1. Introduction

In the 2011 Tohoku Pacific earthquake ($M_w = 9.0$) on March 11 [1], extensive damage to road infrastructure in the Tohoku area occurred because of the accompanying tsunami. Many researchers performed assessments on the vulnerability of structures to tsunami damage for clarifying the relationship between tsunami damage and tsunami wave indices. For instance, Matsutomi and Shuto [2] showed the relationship between the collapse of a house and tsunami wave loads, indicated by indices such as inundation depth and tsunami wave velocity, from the field survey data for the 1993 Hokkaido-Nansei-Oki earthquake tsunami. Shoji and Moriyama [3] evaluated the tsunami fragility curve of a bridge deck subjected to a tsunami wave load, based on a quantitative analysis of the damage data for bridge decks from the 2004 Indian Ocean tsunami in Sri Lanka and Sumatra, Indonesia. Padgett and Spiller [4] developed statistical models for bridge reliability under storm surge loading and validated the failure probability for 44 bridges damaged by the 2005 Hurricane Katrina in North America. Koshimura et al. [5] developed tsunami damage functions for a house by unifying remote sensing data, field survey data, and GIS damage data. Regarding road damage by the 2011 Tohoku Pacific earthquake tsunami, Shoji et al. [6] showed data for road infrastructure damaged by tsunamis and clarified the associated failure modes. Akiyama et al. [7] proposed a framework for estimating the probability of bridge damage to predict the potential tsunami risk, to enhance the promptness in the restoration of transportation facilities. However, the research associated with the development and application of tsunami damage functions for a road bridge remains limited, as described above. In addition, after the Great East Japan earthquake tsunami disaster, it is urgently necessary to determine the tsunami damage risk for road bridges in tsunami hazard areas, particularly areas exposed to anticipated giant plate-boundary and inner-plate earthquakes and tsunamis, such as the Nankai Trough earthquake and tsunami.

Therefore, the authors assessed the tsunami damage to a girder-type road bridge, focusing on the failure of a washed-away deck during the 2011 Tohoku Pacific earthquake tsunami. Based on the data for the washed-away damage ratio, which is defined as the number of washed-away bridges divided by the total number of exposed bridges, damage functions for such bridges are proposed by using three input indices for a tsunami wave load that acts on a road bridge deck having inundation depth h_{ID}, ratio γ of inundation depth h_{ID} compared with the elevation of girder h_g, and flow velocity v_f, as shown in **Fig. 1**. A tsunami waveform with a gently shaped wave-front and water surface level increase rate of less than 2.0 m/min is the focus of this research. In addition, the spatial distribution of physical damage to road bridges by the anticipated Nankai Trough earthquake tsunamis is shown by applying the proposed damage functions.

2. Analytical Method

2.1. Data for Analysis and Definition of Damage Ratio

Damage data obtained by Shoji et al. [6] were analyzed; this included 142 data points on damaged road in-

© Fuji Technology Press Ltd. Creative Commons CC BY-ND: This is an Open Access article distributed under the terms of the Creative Commons Attribution-NoDerivatives 4.0 International License (http://creativecommons.org/licenses/by-nd/4.0/).

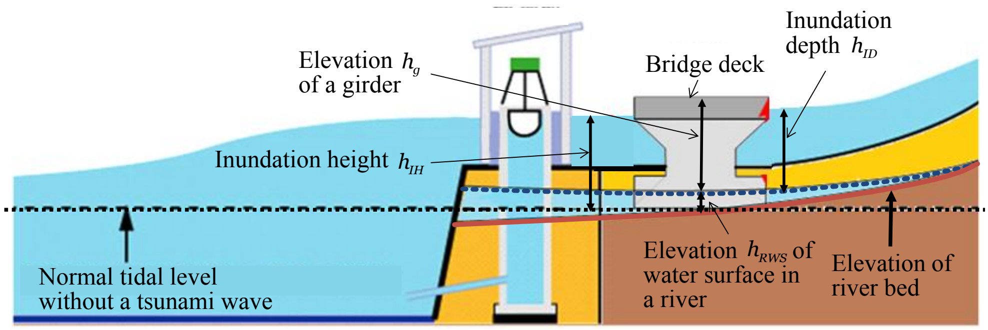

Fig. 1. Definition of inundation height h_{IH}, inundation depth h_{ID}, and ratio γ of inundation depth h_{ID} compared with the elevation of girder h_g. The authors have added the definitions to the figure created by the Geospatial Information Authority of Japan (GSI).

Table 1. Damaged bridges for analysis [6].

Name of Damaged Bridges	Name of Roads	Failure Modes
Waza Bridge	Kadonohama-Tamagawa Line of Iwate Prefectural Route 247	Wash-away of pavement slab and failure of handrail
Hironai Bridge	Noda-Osanai Line of Iwate Prefectural Route 268	Bridge failure
Maita Bridge	National Route 45	Wash-away of embankments of abutments and wash-away of sidewalk bridge
Haipesawa Bridge	Iwaizumi-Hiraga-Fudai Line of Iwate Prefectural Route 44	Wash-away
Namiita Bridge	National Route 45	Failure of abutments
Hinokami Bridge	Kamaishi-Tono Line of Iwate Prefectural Route 35	Deposits
Toyasaka Bridge	National Route 45	Failure of abutments
Katagishi Bridge	National Route 45	Failure of abutments
Kawaharagawa Bridge	National Route 45	Wash-away
Numata-Kosenkyo Bridge	National Route 45	Wash-away
Kesen Bridge	National Route 45	Wash-away
Koizumi Long-bridge	National Route 45	Wash-away
Sodeogawa Bridge	National Route 45	Wash-away of sidewalk bridge
Nijyuuichihama	Bridge National Route 45	Wash-away of embankments of abutments
Utatsu Bridge	National Route 45	Wash-away
Mizushiri Bridge	National Route 45	Wash-away
Oritate Bridge	National Route 398	Wash-away
Yokotsu Bridge	National Route 398	Wash-away
Shinaikawa Bridge	National Route 398	Wash-away
Onosaki Bridge	Kamaya-Osu-Ogatsu Line of Miyagi Prefectural Route 238	Wash-away of embankments of abutments
Onagawa Bridge	National Route 398	Wash-away
Sadakawa Bridge	Ishinomakikougyouko-Yamoto Line of Miyagi Prefectural Route 247	Wash-away
Nonohama Bridge	Onagawa-Oshika Line of Miyagi Prefectural Route 41	Wash-away
Matsugashima Bridge	Okumatsushima-Matsushimakouen Line of Miyagi Prefectural Route 27	Wash-away
Niramori Bridge	Shiogama-Shichigahama-Tagajyo Line of Miyagi Prefectural Route 58	Wash-away
Hashimoto Bridge	Shiogama-Shichigahama-Tagajyo Line of Miyagi Prefectural Route 58	Wash-away
Miyashita Bridge	Yuriagekou Line of Miyagi Prefectural Route 129	Wash-away
Koura Bridge	Soma-Watari Line of Fukushima and Miyagi Prefectural Route 38	Failure of abutments
Otagawa Bridge	National Route 6	Deposits

frastructure, including road embankments and bridges, after the tsunami associated with the 2011 Tohoku Pacific earthquake. For the 142 data points, the authors selected 29 damage data points for girder-type bridges and focused on 17 washed-away girder-type bridges, as given in **Table 1**. In addition to the other 12 data points without

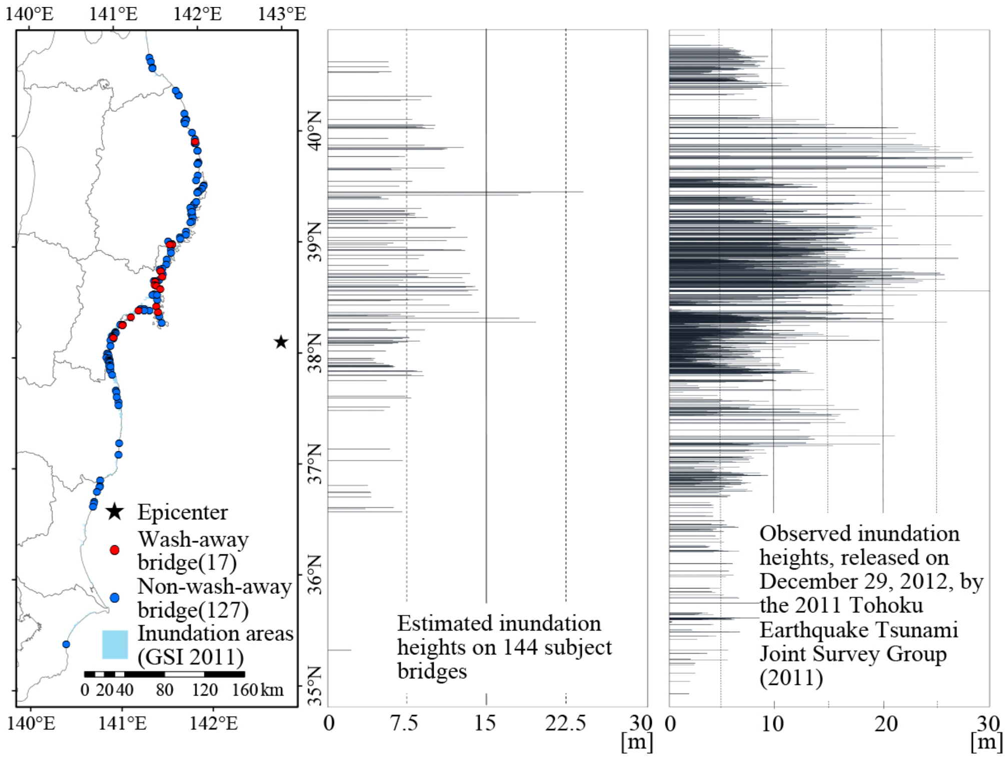

Fig. 2. Locations of subject bridges and the associated inundation heights.

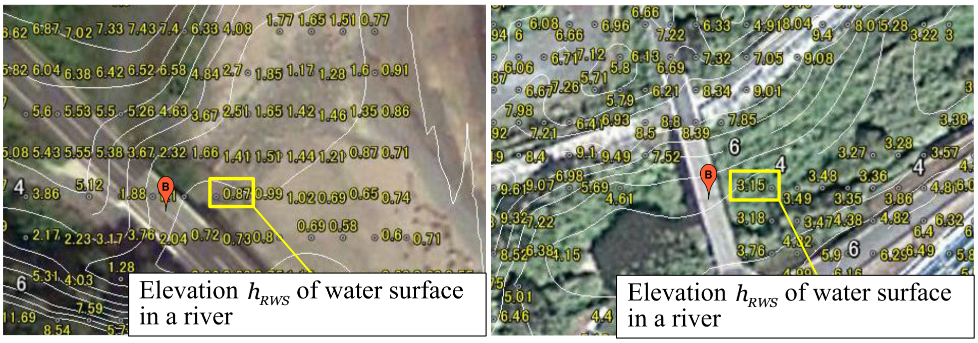

Fig. 3. Analysis of 5-m DEM data for estimating the elevation h_{RWS} of water surface level in a river at a bridge.

wash-away failures, the authors also used the 115 points of non-damage data. In other words, data for 127 non-washed-away girder-type bridges in inundated areas were analyzed in this study. The total number of subject bridges is 144. **Fig. 2** shows the locations of the subject bridges.

For the following analyses, the authors defined the damage ratio of the subject bridges, R_N, as a measure of road bridge damage caused by the tsunamis. R_N is the ratio of the number of washed-away bridges, N_d, divided by the total number of bridges exposed to the tsunami, N_t.

2.2. Data Setting of Inundation Depth, Ratio of Inundation Depth Compared with the Elevation of Girder, and Flow Velocity at a Road Bridge

In calculating h_{ID}, γ, and h_g for a washed-away bridge, we simulated the corresponding inundation heights h_{IH} at the 17 washed-away bridges from 12 series of numerical simulations, as described in the following section, named as simulation group numbers Group 01 to Group 12. The inundation height h_{IH} is defined as the inundated height at a washed-away bridge above the normal tidal level without a tsunami wave, as shown in **Fig. 1**. Meanwhile, in this study, h_{ID} is defined as the distance from the water surface level in the river below a washed-away bridge deck, as shown in **Fig. 1**. Hence, h_{ID} for each washed-away bridge was calculated by subtracting the elevation h_{RWS} of the water surface in the river at the bridge from h_{IH}. The elevation h_{RWS} of the water surface in the river at the bridge was estimated by analyzing the associated 5-m DEM data [8], as shown in **Fig. 3**.

Before calculating these figures, the 127 non-washed-away bridges ($N_t - N_d$) were first classified into two types: 32 non-washed-away bridges with inundation height data observed by the 2011 Tohoku Earthquake Tsunami Joint Survey Group [9] within 250 m of those bridges and 95

Table 2. Number of grids for simulation groups.

Region	Group No.	No. of Grid in x-direction	No. of Grid in y-direction	Grid Size[m]
1	All Groups	480	720	1350
2	All Groups	481	721	450
3	All Groups	481	721	150
4	All Groups	481	721	50
5	All Groups	901	901	16.67(50/3)
6	11	721	1111	5.56(50/9)
	13	1111	721	
	34,35	1201	901	
	38	1201	1201	
	Others	901	901	

bridges without observed inundation height data within 250 m from the bridges. The observed inundation height data with reliability levels A and B, as defined by the 2011 Tohoku Earthquake Tsunami Joint Survey Group for data with high and appropriate reliability levels, respectively, were used for the former 32 bridges, and the inundation height data computed from 32 series of numerical simulations, named simulation group numbers Group 13 to Group 45, were used for the latter 95 bridges. In total, 45 series of numerical simulations for computing h_{IH} at a bridge from Group 01 to Group 45 were performed as described in the following section. In the same manner as that for washed-away bridges, we transferred the observed and simulated h_{IH} data to h_{ID} for non-washed-away bridges by estimating h_{RWS} at the bridge, based on the associated 5-m DEM data [8], as shown in **Fig. 3**.

In calculating the flow velocity v_f at a bridge deck for the 17 washed-away bridges and 127 non-washed-away ones, because of the lack of observed data for v_f at the bridges, we used the data simulated for the bridges from the 45 series of numerical simulations.

In addition, only a tsunami waveform with a gentle wave-front shape having an increase rate of surface water level less than or equal to 2 m/min [10] was selected to model the damage functions. Therefore, the total number of subject bridges was decreased from 144 to 108.

2.3. Model of Damage Function

R_N is expressed as a function of the tsunami wave load index z, the inundation depth h_{ID}, ratio γ of inundation depth h_{ID} compared with the elevation of girder h_g, and the flow velocity v_f at a road bridge. This is described by the damage function modeled by the logarithmic normal cumulative distribution function, as shown in the following equation:

$$R_N(z) = \Phi\left(\frac{\ln z - \lambda}{\zeta}\right) \quad \text{. . . . . (1)}$$

where λ and ζ are the expected value and standard deviation of $\ln z$, respectively. These values are calculated by obtaining the linear regression line between $\Phi^{-1}(R_N)$ and $\ln z$ based on the least-squares method. Φ indicates the standard normal distribution function.

3. Numerical Simulation of Inundation Height at Road Bridge

Simulation groups from Group 01 to Group 45, dependent on the locations of the subject bridges, were set. For each simulation group, the tsunami flow was computed using TUNAMI-CODE [11], and the corresponding inundation heights, h_{IH} at the subject bridges were computed. The governing equations are based on the following three equations using shallow water theory. The equations are discretized by using the finite difference method with a staggered leap-flog scheme.

$$\frac{\partial \eta}{\partial t} + \frac{\partial M}{\partial x} + \frac{\partial N}{\partial y} = 0 \quad \text{. . . . . (2.a)}$$

$$\frac{\partial M}{\partial t} + \frac{\partial}{\partial x}\left(\frac{M^2}{D}\right) + \frac{\partial}{\partial y}\left(\frac{MN}{D}\right) = -gD\frac{\partial \eta}{\partial x} - \frac{gn^2}{D^{7/3}} M\sqrt{M^2+N^2} \quad \text{. (2.b)}$$

$$\frac{\partial N}{\partial t} + \frac{\partial}{\partial x}\left(\frac{MN}{D}\right) + \frac{\partial}{\partial y}\left(\frac{N^2}{D}\right) = -gD\frac{\partial \eta}{\partial y} - \frac{gn^2}{D^{7/3}} N\sqrt{M^2+N^2} \quad \text{. (2.c)}$$

where η is the height of the tsunami wave, and M and N are the flow fluxes in the x and y directions, respectively. The x direction denotes the transverse, while the y direction is longitudinal for a bridge deck. D is the total water depth, which is defined as the summation of the tsunami wave height η and the still water level h. The value of the Manning roughness coefficient n was set as 0.025 for all simulation groups. For each simulation group, six computational regions from Region 1 to Region 6 were used in the nested-grid system. **Table 2** mentions the number of grids in the x and y directions in a WGS-1984-UTM-54-N coordinate system.

Region 1 was the same for all simulation groups. The other regions were defined separately for each simulation group. Region 1 was generated by using global topography data within 30 arc-seconds as collected by GEBCO [12] with a grid size of 1,350 m. Regions

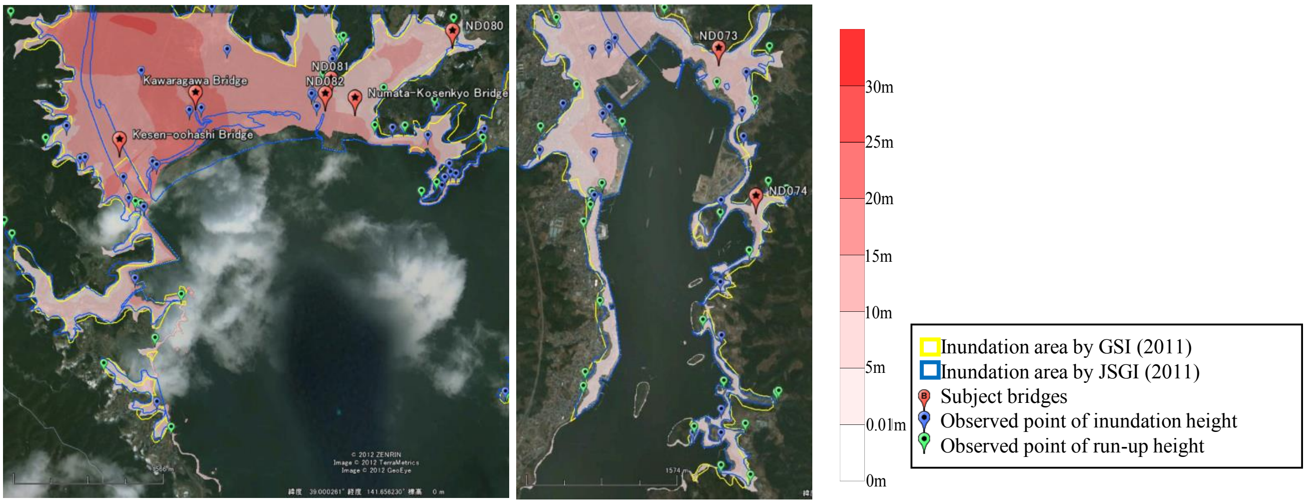

(a) Group 08 simulation (b) Group 27 simulation

Fig. 4. Inundation areas for Group 08 and Group 27 simulations.

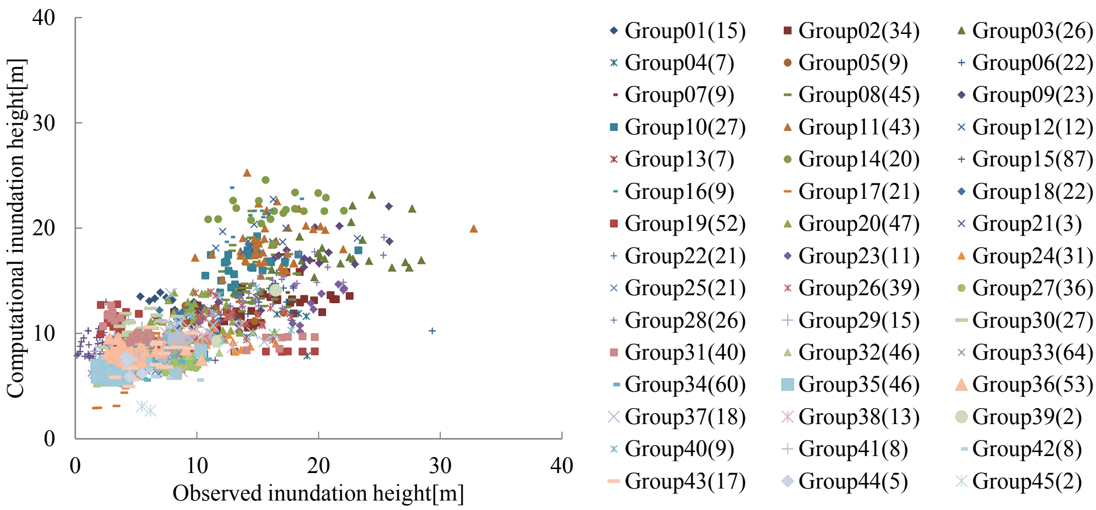

Fig. 5. Comparison of observed inundation heights with simulated inundation heights for each simulation group (Numbers in brackets are the numbers of observation points).

2, 3, and 4 were generated by using 30 arc-second global topography data and 1-m-increment line data for bathymetry [13] with grid sizes of 450 m, 150 m, and 50 m, respectively. Regions 5 and 6 were generated by using 10-m-point DEM data for topography [14] and 1-m-increment line data for bathymetry [13] with grid sizes of 16.67 (50/3) m and 5.56 (50/9) m. The time step for computation was set to 0.10 s, and the total computational time was 180 min or 3 h. The tsunami source model proposed by Fujii et al. [15] was used. The initial water level based on the tsunami source model was determined using Okada's method [16].

The inundation areas were validated by comparing the simulated inundation data with the observed data. **Fig. 4** shows the simulated inundation areas for the Group 08 and Group 27 simulations having two types of observed inundation areas [17, 18]. **Fig. 4(a)** also shows the positions of six subject bridges and the related 45 observation points selected by the 2011 Tohoku Earthquake Tsunami Joint Survey Group [9] with reliabilities A and B for Group 08. Similarly, **Fig. 4(b)** shows the positions of two subject bridges and 36 observation points for Group 27.

Figure 5 shows the relationships between the simulated inundation height data from Group 01 to Group 45 simulations and the observation data. In addition, the authors evaluated the validity of the tsunami simulation scheme using the values of K and κ obtained by the following two formulas [19].

$$\log K = \frac{1}{n_{ob}} \sum_{i=1}^{n_{ob}} \log K_i \quad \text{(3.a)}$$

$$\log \kappa = \sqrt{\frac{1}{n_{ob}} \sum_{i=1}^{n_{ob}} (\log K_i)^2 - (\log K)^2} \quad \text{(3.b)}$$

where K_i is obtained by dividing the value of the observed

Table 3. Values of K and κ for each simulation group (n is number of observed sites).

Group No.	n	K	κ	Group No.	n	K	κ	Group No.	n	K	κ	Group No.	n	K	κ	Group No.	n	K	κ
Group01	15	0.849	1.137	Group10	27	0.942	1.074	Group19	52	0.811	1.329	Group28	26	1.064	1.053	Group37	18	0.984	1.133
Group02	34	1.095	1.094	Group11	43	0.940	1.086	Group20	47	0.926	1.111	Group29	15	0.726	1.202	Group38	13	0.987	1.113
Group03	26	1.080	1.083	Group12	12	0.903	1.078	Group21	3	1.039	1.064	Group30	27	0.763	1.149	Group39	2	1.088	1.017
Group04	7	1.239	1.077	Group13	7	0.891	1.167	Group22	21	0.836	1.172	Group31	40	0.839	1.326	Group40	9	1.004	1.109
Group05	9	1.032	1.102	Group14	20	0.882	1.081	Group23	11	1.185	1.079	Group32	46	0.785	1.177	Group41	8	0.963	1.089
Group06	22	1.039	1.146	Group15	87	0.818	1.204	Group24	31	1.021	1.148	Group33	64	0.721	1.208	Group42	8	1.011	1.133
Group07	9	1.011	1.069	Group16	9	0.848	1.047	Group25	21	1.024	1.079	Group34	60	0.798	1.194	Group43	17	0.917	1.096
Group08	45	0.990	1.078	Group17	21	0.895	1.083	Group26	39	1.038	1.094	Group35	46	0.770	1.164	Group44	5	0.836	1.086
Group09	23	1.016	1.073	Group18	22	0.886	1.090	Group27	36	1.075	1.054	Group36	53	0.776	1.130	Group45	2	1.367	1.059

inundation height h^i_{IHob} by the value of the simulated inundation height h^i_{IHsm} at the observation point i. n_{ob} is the total number of observed points.

Table 3 gives the comparison of the simulated data with the observed data for the 45 simulation groups. The total number of observed points n_{ob} is 1,179. The variation of K from 0.721 to 1.367 and of κ from 1.017 to 1.329 supports the validity of the 45 series of simulations of the tsunami wave and inundation height [20]. Based on this validation, the simulated inundation height data at a given subject bridge can be used as the input inundation height acting on the bridge deck, considering the accuracy of the simulated results shown in **Fig. 5** and **Table 3**.

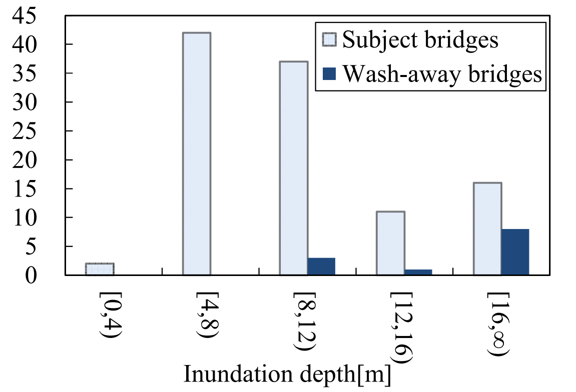

Fig. 6. Frequency of bridge data dependent on inundation depth h_{ID}.

4. Trends of Damage Ratio and Development of Damage Functions

4.1. For Index 1: inundation depth h_{ID}

Figure 6 shows the frequency of the bridge data for 108 of the total number of subject bridges N_t dependent on inundation depth h_{ID}, including both washed-away and non-washed-away bridges. These data were classified in a 4-m-interval of inundation depth h_{ID}. N_t, with the inundation depth range h_{ID} of 4.0 m to 8.0 m, shows the largest value of 42. **Fig. 6** also shows the frequency of the number of wash-away bridges, N_d, dependent on the inundation depth h_{ID}. These data were also classified in the same interval. N_d, with inundation depths h_{ID} exceeding 16.0 m, has the largest value of 8.

The damage ratio R_N was calculated at 2.0-m intervals in the inundation depth h_{ID}. **Fig. 7** shows the relationship between the damage ratio R_N and inundation depth h_{ID}. **Fig. 7** also shows the same relationship for the 2004 Indian Ocean tsunami data by Shoji and Moriyama [3]. From **Fig. 7**, R_N with inundation depth h_{ID} of 2.0 m is zero, R_N with inundation depth h_{ID} of 6.0 m to 10.0 m increases slightly to 0.024–0.028, and R_N with inundation depth h_{ID} of 14.0 m increases to 0.167, which indicates severe damage to road infrastructure. R_N with inundation depth h_{ID} of 18.0 m increases to the largest value of 0.50, which indicates the extremity of the situation involving road infrastructure damage by tsunamis. The highest R_N is observed at Rikuzentakata in Iwate Prefecture for the

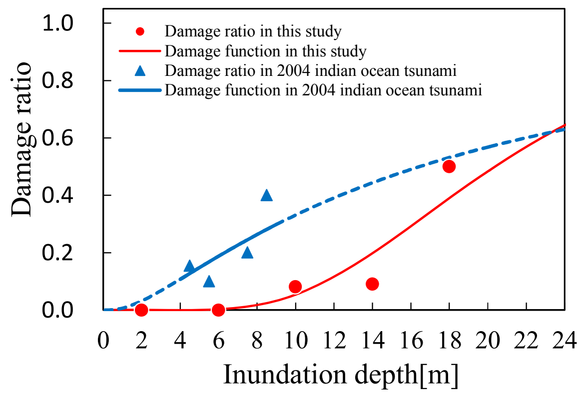

Fig. 7. Relationship between damage ratio and inundation depth h_{ID}.

Kawaharagawa and Kesen Bridges (Group 08); Minami-Sanriku, Motoyoshi district in Miyagi Prefecture for the Utatsu, Mizushiri, and Yokotsu Bridges (Group 10 and Group 11); Ishinomaki in Miyagi Prefecture for the Shin-Aikawa Bridge (Group 12); and Onagawa in Miyagi Prefecture for the Onagawa Bridge (Group 17).

Finally, the tsunami damage function R_N, dependent on the inundation depth h_{ID} and describing the occurrence of wash-away failure for a road bridge deck, was deduced as shown in **Fig. 7**, and the following equation was obtained.

$$R_N(h_{ID}) = \Phi\left(\frac{\ln h_{ID} - 3.01}{0.44}\right) \quad \cdots\cdots\cdots (4)$$

Table 4. Identified parameters of damage functions in a wash-away failure mode for a girder-type road bridge.

	Inundation depth		γ	Inundation depth
	This study	The 2004 indian ocean tsunami[3]	This study	This study
Inclination	2.26	0.88	0.91	0.78
Intercept	-6.81	-2.46	-0.50	-2.53
Coefficient of determination R^2	0.71	0.79	0.96	0.86
Excepted value[m]	22.47	31.49	3.19	59.53
Median mz[m]	20.37	16.37	1.74	26.04
Standard diviation σ_z [m]	10.46	51.44	4.91	122.40

Another damage function of the inundation depth h_{ID} was developed based on the analysis of bridge damage data for the 2004 Indian Ocean tsunami, as shown in **Fig. 7** [3]. **Table 4** shows the associated parameters of both damage functions. From **Fig. 7**, the damage ratio calculated by the model in this study shows low values compared to those calculated using the 2004 Indian Ocean tsunami data. These bridge decks, exposed to the 2004 Indian Ocean tsunami and located on Sumatra Island in Indonesia, were not completely fixed to the piers or at both abutments by bearings. Meanwhile, the subject bridge decks in this study located in Tohoku were designed with upward resistances of 30% of the dead load of the superstructure in the vertical direction, using bearings. Therefore, it is estimated that the bridge decks addressed in this study are more robust than those exposed to the 2004 Indian Ocean tsunami against wash-away failure, based on comparing the damage functions.

4.2. For Index 2: Ratio γ of Inundation Depth Compared with Girder Elevation

To form a physically reasonable damage function reflecting the wash-away failure mechanism of a road bridge deck caused by a tsunami surge wave, it is necessary to consider the parameters of the tsunami wave height at a given bridge site as well as the girder height compared to the wave height. Hence, the meaning of the ratio γ of the inundation depth h_{ID} compared with the girder elevation h_g was clarified in the following equation.

$$\gamma = \frac{h_{ID} - h_g}{h_{ID}} \quad \text{. . . . . (5)}$$

Figure 8 shows the frequency of the total number of subject bridges N_t dependent on γ, classified in a 0.2 m/m interval. N_t with γ of 0.6 m/m to 0.8 m/m shows the largest value of 29. **Fig. 8** also shows the frequency of the number of wash-away bridges N_d as a function of γ in the same interval. N_d with γ of 0.8 m/m to 1.0 m/m shows the largest value of 6.

Figure 9 shows the relationship between the damage ratio R_N and γ. From **Fig. 9**, R_N with γ of 0.1 m/m is zero; R_N with γ of 0.3 m/m increases slightly to 0.059; and R_N with γ of 0.7 m/m reaches the value of 0.172, which indicates a probability of failure approaching 20%. This corresponds to extremely severe damage to the road infrastructure. R_N with γ of 0.9 m/m increases to the largest value of 0.261.

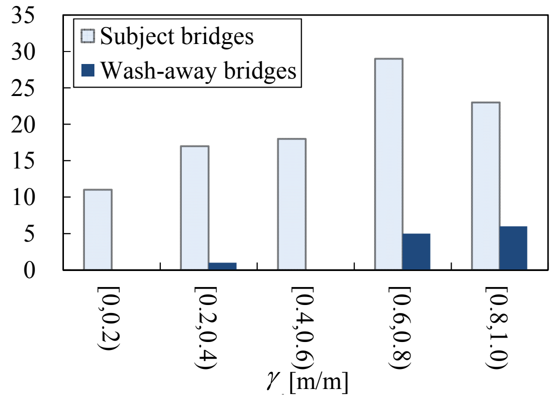

Fig. 8. Frequency of bridge data dependent on ratio γ of inundation depth h_{ID} compared with the elevation of girder h_g.

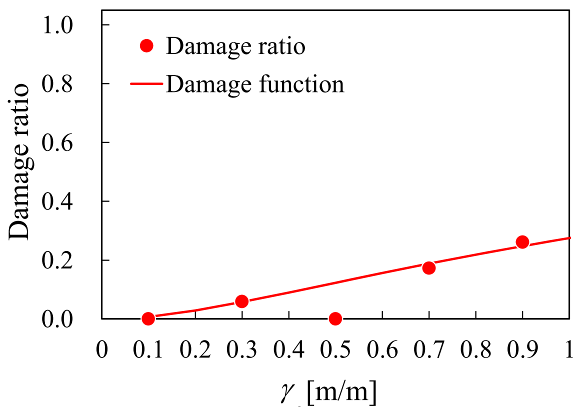

Fig. 9. Relationship between damage ratio and ratio γ of inundation depth h_{ID} compared with the elevation of girder h_g.

Figure 9 and **Table 4** also show the proposed damage function R_N dependent on γ and the associated parameters based on these calculated damage ratios. The damage function is formulated by the following equation.

$$R_N(\gamma) = \Phi\left(\frac{\ln \gamma - 0.74}{1.23}\right) \quad \text{. . . . . (6)}$$

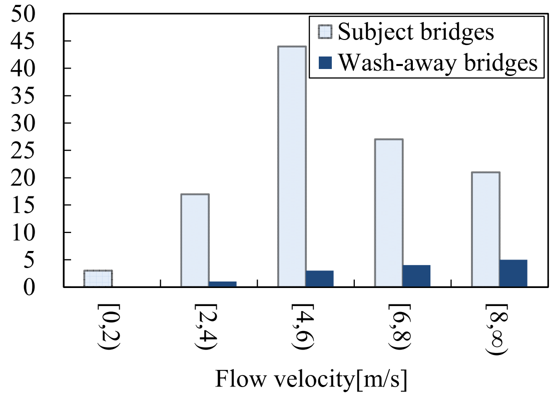

Fig. 10. Frequency of bridge data dependent on flow velocity.

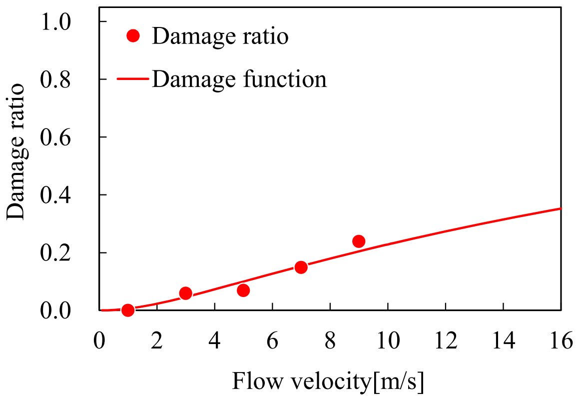

Fig. 11. Relationship between damage ratio and flow velocity.

4.3. For Index 3: Flow Velocity v_f

Figure 10 shows the frequency of the total number of subject bridges N_t dependent on flow velocity v_f in a 2.0 m/s interval. N_t with v_f of 4.0 m/s to 6.0 m/s shows the largest value of 44. **Fig. 10** also shows the frequency of the number of wash-away bridges N_d. N_d with v_f exceeding 8.0 m/s shows the largest value of 5.

From the calculation of the damage ratio, R_N, based on the frequency data, the relationship between the damage ratio R_N and flow velocity v_f was derived in **Fig. 11**. From **Fig. 11**, R_N with v_f of 1.0 m/s is zero, while R_N with v_f of 3.0 m/s to 5.0 m/s shows a relatively low probability of failure from 0.059 to 0.068. Beyond this flow velocity level, R_N with v_f of 7.0 m/s increases to 0.148, and R_N with v_f of 9.0 m/s increases to the largest value of 0.238, corresponding to extremely severe damage of the road bridge deck.

Figure 11 also shows a proposed alternative damage function R_N based on these calculated damage ratios dependent on flow velocity v_f. **Table 4** again gives the associated parameters. From the perspective of v_f, the damage function is modeled by the following formulation.

$$R_N\left(v_f\right) = \Phi\left(\frac{\ln v_f - 3.26}{1.29}\right) \quad \ldots\ldots\ldots \quad (7)$$

5. Estimation of Wash-Away Road Bridge Damage in the Nankai Trough Earthquake and Tsunami

5.1. Data Set

Wash-away damage to road bridge decks subjected to the anticipated Nankai Trough earthquake tsunami was estimated by applying the proposed damage functions, using data for the inundation depths h_{ID} provided by the Cabinet Office of the Government of Japan [21]. The three tsunami source models were anticipated. **Fig. 12** shows the spatial distribution of the estimated inundation depths for each case. The road bridges were selected from expressways, national roads, prefectural roads, and city roads located on the targeted coasts; data characterizing the bridges were provided by the road network data [22].

The road network data does not contain the girder elevation h_g, and the data offered by the Cabinet Office of the Government of Japan does not contain the flow velocity v_f. Hence, in this section, we apply the damage function by the inundation depth h_{ID}, as in Eq. (4), for the following case studies.

5.2. Discussion for Case Studies

The wash-away damage for exposed road bridge decks by three simulated tsunami inundations in the case of setting high-slip subfaults in Suruga Bay to Kii Peninsula (Case 1), off the coast of Shikoku to Kyushu (Case 2) and off Aichi Prefecture to Mie Prefecture and Muroto Cape (Case 3) were estimated. The number of exposed road bridges is 5,458, 5,440, and 5,440, respectively, for Cases 1 to 3. **Fig. 13** shows the frequency of subject bridges as a function of inundation depth h_{ID}, and **Fig. 14** shows the spatial distribution of the inundation depth at each bridge for each case. By substituting the values of the anticipated inundation depth h_{ID} for each case into the proposed damage function in Eq. (4), the spatial distribution of the damage ratio $R_N\left(h_{ID}\right)$ is derived in **Fig. 15**. In addition, the frequency of subject bridges dependent on damage ratio $R_N\left(h_{ID}\right)$ is also computed for each case in **Fig. 16**.

These damage estimations reveal the characteristics of spatial damage classification for the wash-away failures of road bridges distributed along a coast in response to an anticipated tsunami. Case 2 was found to be the worst scenario. Case 3 was the second worst and Case 1 was a scenario with a relatively minor effect, showing the spatial spreading of wash-away road bridge damage from Okinawa to Ibaraki Prefecture. For Case 2, showing values of damage ratio $R_N\left(h_{ID}\right)$ higher than or equal to 0.10 along the coasts of Kyushu, Shikoku, and Kii Peninsula, the bridge decks distributed in Kuroshio, Susaki, and Tosashimizu in Kochi Prefecture, in Saiki in Oita Prefecture, and in Susami in Wakayama Prefecture could be most severely affected. Based on these estimations, we can proceed to the next risk assessment, focusing on the washing away of road bridges and estimating the functional loss of road networks in the areas with high wash-away probabilities.

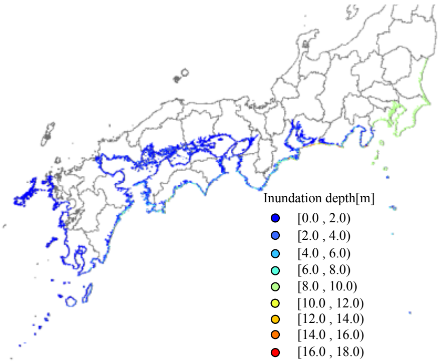

(a) For Case 1

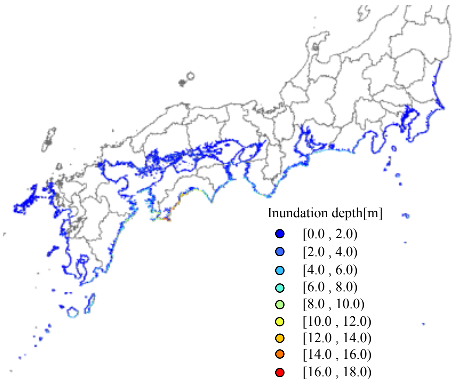

(b) For Case 2

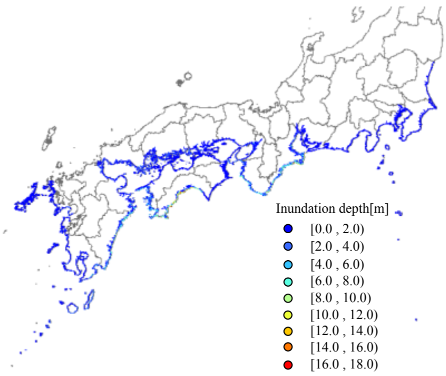

(c) For Case 3

Fig. 12. Spatial distribution of simulated inundation depths in the anticipated Nankai Trough earthquake tsunami.

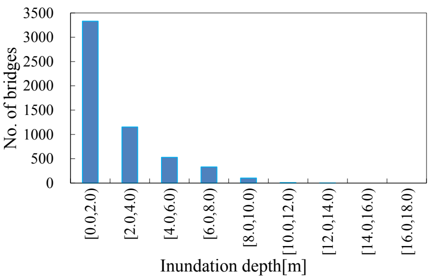

(a) For Case 1

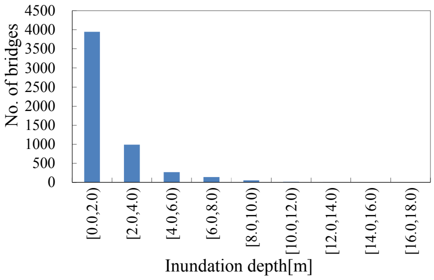

(b) For Case 2

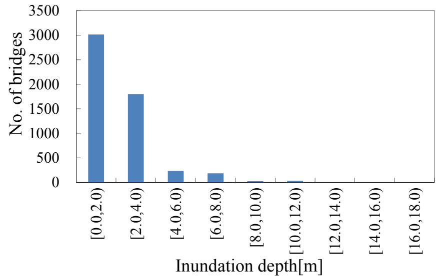

(c) For Case 3

Fig. 13. Frequency of estimated road bridge data with inundation depth in the anticipated Nankai Trough earthquake tsunami.

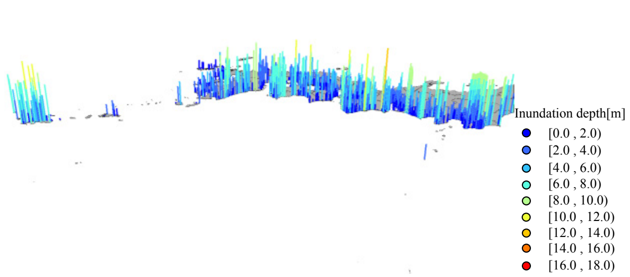

(a) For Case 1

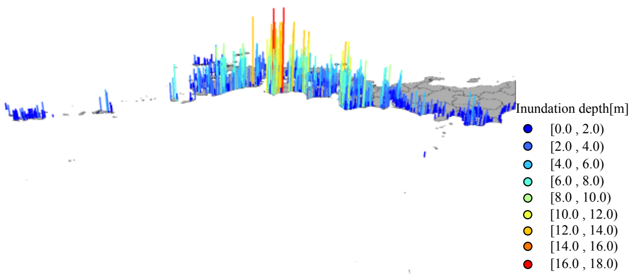

(b) For Case 2

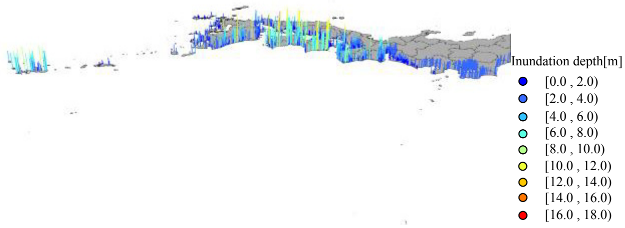

(c) For Case 3

Fig. 14. Spatial distribution of estimated road bridges with inundation depth in the anticipated Nankai Trough earthquake tsunami.

6. Conclusions

Tsunami damage on girder-type road bridges, focusing on wash-away deck failures caused by the 2011 Tohoku Pacific earthquake tsunami was assessed. The inundation depth h_{ID}, ratio γ of inundation depth h_{ID} compared with the elevation of girder h_g, and flow velocity v_f were selected as the three indices to measure the tsunami wave load acting on a road bridge deck. Tsunami waveforms with gently shaped wave-fronts, increasing rates of water surface level by less than or equal to 2.0 m/min were selected for investigation. The damage ratio R_N was computed for the above three indices and defined by the number of washed-away bridges divided by the total number of bridges exposed to the tsunami.

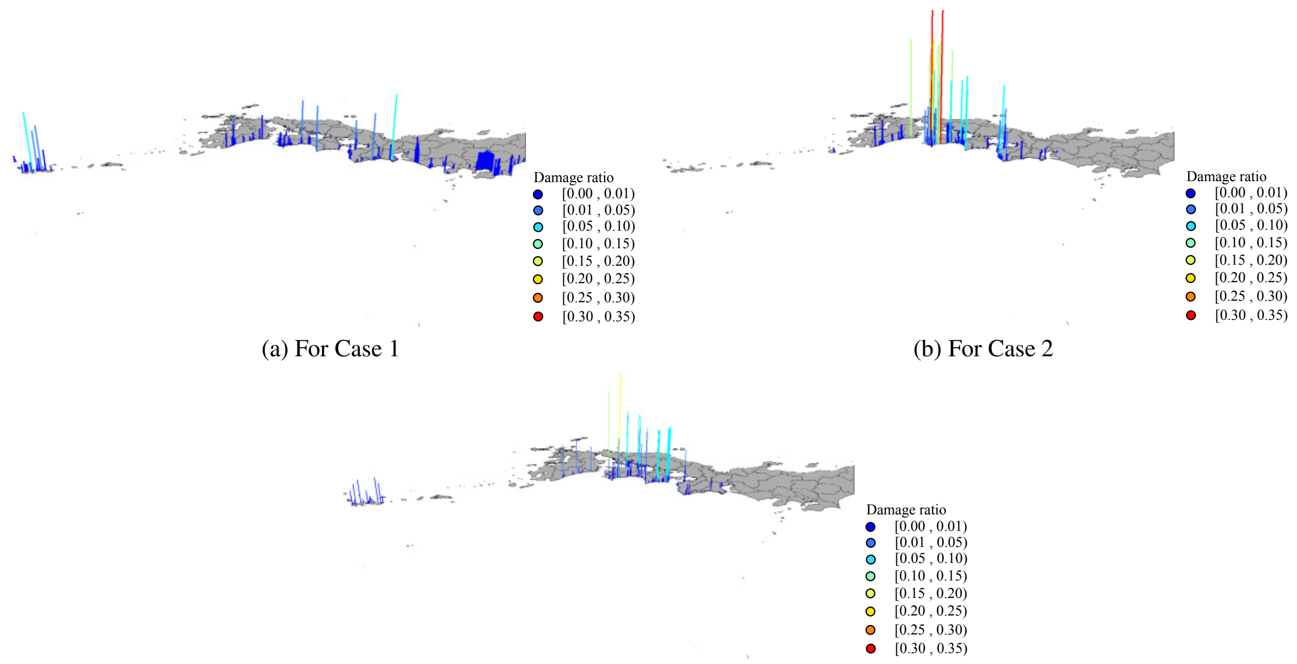

(a) For Case 1 (b) For Case 2 (c) For Case 3

Fig. 15. Spatial distribution of estimated road bridges with damage ratio by the anticipated Nankai Trough earthquake tsunami.

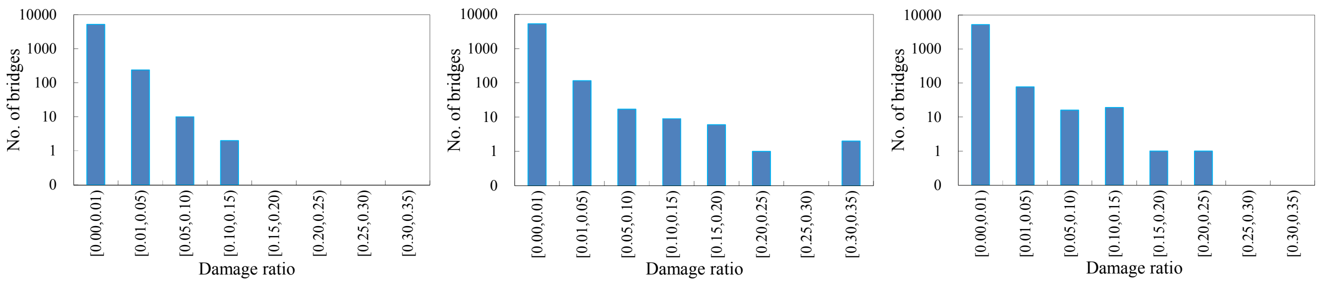

(a) For Case 1 (b) For Case 2 (c) For Case 3

Fig. 16. Frequency of estimated road bridge data with damage ratio by the anticipated Nankai Trough earthquake tsunami.

Based on statistical analyses of the data regarding the damage ratio R_N, the damage functions by the three indices of wave load were proposed. In addition, the spatial distributions of the physical wash-away failure of road bridge decks from the anticipated Nankai Trough earthquake tsunami, induced by three higher-slip-subfaulting scenarios, were determined by applying the inundation depth data to one of the proposed damage functions dependent on inundation depth h_{ID}, allowing clarification of potential damage trends.

In future, the values of girder elevation h_g at each bridge site may provide more accuracy by improving the associated data settings for the DEM around a bridge. The other two damage functions, dependent on the ratio γ of inundation depth h_{ID} compared with the elevation of girder h_g and the flow velocity v_f, as described in Eqs. (6) and (7), should be applied for further case studies to complement the lack of observed data.

Acknowledgements

The authors specially acknowledge the valuable support for the numerical simulation in calculating inundation heights at the subject bridges from the International Research Institute of Disaster Science, Tohoku University (Professor F. Imamura and Professor S. Koshimura). This study was sponsored by the Integrated Risk Management Project for Complex Disasters on Large-scale Earthquakes at the University of Tsukuba (Leader: Associate Professor Y. Yagi, Division leader: Associate Professor G. Shoji). This research was also sponsored in part by the Ministry of Education, Culture, Sports, Science, and Technology (MEXT) under "Special Project on Reducing Vulnerability for Urban Mega Earthquake Disasters" (Head: Professor H. Hayashi at DPRI, Kyoto University and Division leader Professor N. Nojima at Gifu University). The authors are most grateful to Associate Professor Y. Maruyama at Chiba University for providing road network data. The authors also would like to give special and sincere thanks to Mr. K. Takahashi, Mr. Y. Ezura, Mr. H. Takahashi, and Mr. N. Ishikawa, who are former doctoral, undergraduate, and graduate students at the University of Tsukuba, for calculating inundation heights and depths at the damaged bridges.

References:

[1] Japan Meteorological Agency (JMA), "The 2011 Great East Japan Earthquake ∼first report∼," 2016, http://www.jma.go.jp/jma/en/News/2011_Earthquake_01.html [accessed August 11, 2016]

[2] H. Matsutomi and N. Shuto, "Inundation Depth Due to a Tsunami and Houses," Procs. of Coastal Engineering, Japan Society of Civil Engineers (JSCE), Vol.41, pp. 246-250, 1994 (in Japanese).

[3] G. Shoji and T. Moriyama, "Evaluation of the Structural Fragility of a Bridge Structure Subjected to a Tsunami Wave Load," J. of Natural Disaster Science, Vol.29, No.2, pp. 73-81. 2007.

[4] J. E. Padgett and A. Spiller, "Empirical Evidence from Hurricane Katrina on the Failure Probability of Bridges under Storm Surge Loading," Procs. of the 10th Int. Conf. on Structural Safety and Reliability (ICOSSAR), Osaka, Japan, September, 2009.

[5] S. Koshimura, Y. Namegaya, and H. Yanagisawa, "Fragility Functions for Tsunami Damage Estimation," J. of Hydraulic, Coastal and Environmental Engineering (B), Japan Society of Civil Engineers (JSCE), Vol.65, No.4, pp. 320-331, 2009 (in Japanese).

[6] G. Shoji, T. Nakamura, and K. Takahashi, "Tsunami Damage Assessment on Road Structures in the 2011 off the Pacific Coast of Tohoku Earthquake," Proc. of the Int. Symposium on Engineering Lessons Learned from the 2011 Great East Japan Earthquake, pp. 1711-1721, 2012.

[7] M. Akiyama, D. M. Frangopol, M. Arai, and S. Koshimura, "Reliability of Bridges under Tsunami Hazards: Emphasis on the 2011 Tohoku-Oki Earthquake," Earthquake Spectra, Vol.29, No.S1, pp. S295-S314, 2013.

[8] Geospatial Information Authority of Japan (GSI), "The Base Map Information Download Service," 5m Interval DEM Data, 2012 (in Japanese), http://fgd.gsi.go.jp/download/ [accessed August 11, 2016]

[9] The 2011 Tohoku Earthquake Tsunami Joint Survey Group, "The 2011 off the Pacific Coast of Tohoku Earthquake Tsunami Information," Results of Tsunami Surveys, 2011, http://www.coastal.jp/tsunami2011/ [accessed August 11, 2016]

[10] T. Nakamura and G. Shoji, "Clarification of Tsunami Waveforms Acting on a Bridge Structure Subjected to the 2011 off the Pacific Coast of Tohoku Earthquake Tsunami," J. of Structural Engineering & Earthquake Engineering (A1), Japan Society of Civil Engineers (JSCE), Vol.70, No.4, pp. I_210-I_218, 2014 (in Japanese).

[11] S. Koshimura, "TUNAMI-CODE Tohoku University's Numerical Analysis Model for Investigation of Tsunami," Disaster Control Research Center (DCRC), Tohoku University, 2009.

[12] The British Oceanographic Data Centre (BODC), "The General Bathymetry Chart of the Oceans (GEBCO)," The GEBCO_08 Grid, 2008, http://www.gebco.net/ [accessed August 11, 2016]

[13] Japan Hydraulic Association (JHA), "Digital Topography of Ocean Floor M7000 Series," Contour Maps, 2011 (in Japanese).

[14] Geospatial Information Authority of Japan (GSI), "The Base Map Information Download Service," 10m Interval DEM Data, 2012 (in Japanese), http://fgd.gsi.go.jp/download/ [accessed August 11, 2016]

[15] Y. Fujii, K. Satake, S. Sakai, M. Shinohara, and T. Kanazawa, "Tsunami Source of the 2011 off the Pacific Coast of Tohoku Earthquake," Earth Planets Space, Vol.63, pp. 815-820, 2011.

[16] Y. Okada, "Surface Deformation Due to Shear and Tensile Faults in a Half-Space," Bulletin of the Seismological Society of America, Vol.75, pp. 1135-1154, 1995.

[17] Geospatial Information Authority of Japan (GSI), "Inundation Area Maps," 2011 (in Japanese), http://www.gsi.go.jp/kikaku/kikaku60003.html [accessed August 11, 2016]

[18] Japan Society of Geoinformatics (JSGI), "2011 Tsunami in East Japan," Inundation Areas, 2012, http://www.jsgi-map.org/tsunami/google_tile_en.html [accessed August 11, 2016]

[19] The Tsunami Evaluation Subcommittee, "Tsunami Assessment Method for Nuclear Power Plants in Japan," Method for Verifying the Assessment Procedure Based on Historical Tsunamis, The Nuclear Civil Engineering Committee, Japan Society of Civil Engineers (JSCE), 2012, http://committees.jsce.or.jp/ceofnp/system/files/JSCE_Tsunami_060519.pdf [accessed August 11, 2016]

[20] I. Aida, "Numerical Experiments of Historical Tsunamis Generated off the Coast of the Tokaido District," Bulletin of the Earthquake Research Institute, University of Tokyo, Vol.56, No.2, pp. 367-390, 1981 (in Japanese).

[21] Cabinet Office, Government of Japan, "Damage Estimation in the Nankai Trough Earthquake," 2012 (in Japanese), http://www.bousai.go.jp/jishin/nankai/model/index.html [accessed August 11, 2016]

[22] Orkney, Inc., Road Network Data, 2009 (in Japanese).

Name:
Gaku Shoji

Affiliation:
Associate Professor, Division of Engineering Mechanics and Energy, Faculty of Engineering, Information and Systems, University of Tsukuba

Address:
1-1-1 Tennodai, Tsukuba, Ibaraki 305-8573, Japan

Brief Career:
1996- Research Associate, Tokyo Institute of Technology
2001- Assistant Professor, University of Tsukuba
2008- Associate Professor, University of Tsukuba

Selected Publications:
• "Development of Damage Functions on Water Supply Systems subjected to an Extreme Ground Motion," Procs. of the 11th Int. Conf. on Structural Safety and Reliability (ICOSSAR2013), New York, USA, Safety, Reliability, Risk and Life-Cycle Performance of Structures & Infrastructures eds by G. Deodatis, B. R. Ellingwood and D. M. Frangopol, CRC Press Taylor & Francis Group, London, ISBN 978-1-138-00086-5, pp. 691-698 , June, 2013.

Academic Societies & Scientific Organizations:
• Japan Society of Civil Engineers (JSCE)
• Japan Association for Earthquake Engineering (JAEE)
• Institute of Social Safety Science (ISSS)

Name:
Tomoharu Nakamura

Affiliation:
Former Graduate Student, Graduate School of Systems and Information Engineering, University of Tsukuba

Address:
1-1-1 Tennodai, Tsukuba, Ibaraki 305-8573, Japan

Brief Career:
2014- Master of Engineering, Graduate School of Systems and Information Engineering, University of Tsukuba
2014- West Japan Railway Company

Selected Publications:
• "Development of Damage Functions on Road Infrastructures Subjected to Extreme Ground Excitations by Analyzing Damage in the 2011 off the Pacific Coast of Tohoku Earthquake," J. of Disaster Research, Vol.9, No.2, pp. 121-127, 2014.

Academic Societies & Scientific Organizations:
• Japan Society of Civil Engineers (JSCE)